

Muscle size explains low passive skeletal muscle force in heart failure patients

Fausto Antonio Panizzolo ^{Corresp., 1, 2}, Andrew J Maiorana ^{3, 4}, Louise H Naylor ², Lawrence G Dembo ⁵, David G Lloyd ⁶, Daniel J Green ^{2, 7}, Jonas Rubenson ^{2, 8}

¹ John A. Paulson School of Engineering and Applied Sciences, Harvard University, Cambridge, MA, United States

² The School of Sport Science, Exercise and Health, The University of Western Australia, Crawley, WA, Australia

³ Advanced Heart Failure and Cardiac Transplant Service, Royal Perth Hospital, Perth, WA, Australia

⁴ School of Physiotherapy and Exercise Science, Curtin University, Perth, WA, Australia

⁵ Envision Medical Imaging, Perth, WA, Australia

⁶ Centre for Musculoskeletal Research, Griffith Health Institute, Griffith University, Gold Coast, QLD, Australia

⁷ Research Institute for Sport and Exercise Science, Liverpool John Moores University, Liverpool, United Kingdom

⁸ Biomechanics Laboratory, Department of Kinesiology, The Pennsylvania State University, University Park, PA, United States

Corresponding Author: Fausto Antonio Panizzolo

Email address: fpanizzolo@seas.harvard.edu

Background. Alterations in skeletal muscle function and architecture have been linked to the compromised exercise capacity characterizing chronic heart failure (CHF). However, how passive skeletal muscle force is affected in CHF is not clear. Understanding passive force characteristics in CHF can help further elucidate the extent to which altered contractile properties and/or architecture might affect muscle and locomotor function. Therefore, the aim of this study was to investigate passive force in a single muscle for which non-invasive measures of muscle size and estimates of fiber force are possible, the soleus (SOL), both in CHF patients and age- and physical activity-matched control participants. **Methods.** Passive SOL muscle force and size were obtained by means of a novel approach combining experimental data (dynamometry, electromyography, ultrasound imaging) with a musculoskeletal model. **Results.** We found reduced passive SOL forces (~30%) (at the same relative levels of muscle stretch) in CHF vs. healthy individuals. This difference was eliminated when force was normalized by physiological cross sectional area, indicating that reduced force output may be most strongly associated with muscle size. Nevertheless, passive force was significantly higher in CHF at a given absolute muscle length (non length-normalized) and likely explained by the shorter muscle slack lengths and optimal muscle lengths measured in CHF compared to the control participants. This later factor may lead to altered performance of the SOL in functional tasks such gait. **Discussion.** These findings suggest introducing exercise rehabilitation targeting muscle hypertrophy and, specifically for the calf muscles, exercise that promotes muscle lengthening.

1 **Muscle size explains low passive skeletal muscle force in heart**
2 **failure patients**

3
4 Fausto A. Panizzolo^{1,2}, Andrew J. Maiorana^{3,4}, Louise H. Naylor¹, Lawrence Dembo⁵, David G. Lloyd⁶,
5 Daniel J. Green^{1,7}, and Jonas Rubenson^{1,8}

6
7 ¹The School of Sport Science, Exercise and Health, The University of Western Australia, Crawley, WA,
8 Australia.

9 ²John A. Paulson School of Engineering and Applied Sciences, Harvard University, Cambridge, MA,
10 United States.

11 ³Advanced Heart Failure and Cardiac Transplant Service, Royal Perth Hospital, Perth, WA, Australia.

12 ⁴School of Physiotherapy and Exercise Science, Curtin University, Perth, WA, Australia.

13 ⁵Envision Medical Imaging, Perth, WA, Australia.

14 ⁶Centre for Musculoskeletal Research, Griffith Health Institute, Griffith University, Gold Coast, QLD,
15 Australia.

16 ⁷Research Institute for Sport and Exercise Science, Liverpool John Moores University, Liverpool, United
17 Kingdom.

18 ⁸Biomechanics Laboratory, Department of Kinesiology, The Pennsylvania State University, University
19 Park, PA, United States.

20

21 **Corresponding author:** Dr. Fausto A. Panizzolo

22 John A. Paulson School of Engineering and Applied Sciences

23 Harvard University, 60 Oxford st, Cambridge, MA, USA.

24 Email: fpanizzolo@seas.harvard.edu

25

26

27 **ABSTRACT**

28 **Background.** Alterations in skeletal muscle function and architecture have been linked to the
29 compromised exercise capacity characterizing chronic heart failure (CHF). However, how
30 passive skeletal muscle force is affected in CHF is not clear. Understanding passive force
31 characteristics in CHF can help further elucidate the extent to which altered contractile properties
32 and/or architecture might affect muscle and locomotor function. Therefore, the aim of this study
33 was to investigate passive force in a single muscle for which non-invasive measures of muscle
34 size and estimates of fiber force are possible, the soleus (SOL), both in CHF patients and age-
35 and physical activity-matched control participants.

36 **Methods.** Passive SOL muscle force and size were obtained by means of a novel approach
37 combining experimental data (dynamometry, electromyography, ultrasound imaging) with a
38 musculoskeletal model.

39 **Results.** We found reduced passive SOL forces (~30%) (at the same relative levels of muscle
40 stretch) in CHF *vs.* healthy individuals. This difference was eliminated when force was
41 normalized by physiological cross sectional area, indicating that reduced force output may be
42 most strongly associated with muscle size. Nevertheless, passive force was significantly higher
43 in CHF at a given absolute muscle length (non length-normalized) and likely explained by the
44 shorter muscle slack lengths and optimal muscle lengths measured in CHF compared to the
45 control participants. This later factor may lead to altered performance of the SOL in functional
46 tasks such gait.

47 **Discussion.** These findings suggest introducing exercise rehabilitation targeting muscle
48 hypertrophy and, specifically for the calf muscles, exercise that promotes muscle lengthening.

49

50

51 INTRODUCTION

52 Growing evidence suggests that architectural and functional deficiencies (e.g. strength) in the
53 skeletal muscle contribute to the limited ability to perform daily tasks and the overall poor
54 exercise tolerance that characterizes chronic heart failure (CHF) and to the progression of the
55 disease (*Green et al., 2016*). For example, it is apparent that patients with CHF have a reduction
56 in muscle size (*Mancini et al., 1992; Minotti et al., 1993; Anker et al., 1999; Fülster et al., 2013*)
57 and strength (as determined by net joint moments) in the lower limbs (*Magnusson et al., 1994;*
58 *Chua et al., 1995; Harrington et al., 1997; Sunnerhagen et al., 1998; Toth et al., 2006; Toth et*
59 *al., 2010; Panizzolo et al., 2015*) compared to healthy age-matched individuals; these reductions
60 are also related to reductions in aerobic exercise capacity ($\dot{V}O_2$ peak) (*Volterrani et al., 1994;*
61 *Harrington et al., 1997; Panizzolo et al., 2015*). It is still not clear, however, if the reduction in
62 muscle function and aerobic capacity are associated primarily with reduced muscle size that is
63 known to occur in CHF (*Mancini et al., 1992; Fülster et al., 2013; Panizzolo et al., 2015*) or if
64 size-independent characteristics is an important determinant. Indeed, several studies that have
65 measured both voluntary strength and muscle size in the quadriceps suggest that muscle size
66 alone does not account for the loss of strength (*Harrington et al., 1997; Toth et al., 2006; Toth et*
67 *al., 2010*). Resolving whether muscle size or other size-independent muscle properties are more
68 closely linked to muscle function can prove important for guiding rehabilitation strategies in
69 CHF.

70 To this extent, measurements of passive muscle forces and how they are related to muscle
71 architecture can provide important information for understanding the mechanisms behind the
72 alterations in skeletal muscle function associated with CHF. In particular, they can shed further
73 light on whether skeletal muscle deficits at a whole muscle level are related primarily to

74 reductions in muscle size without introducing variability arising from voluntary and/or twitch
75 contractions (*Princivero et al., 2000; Oskouei et al., 2003*). Passive forces are also functionally
76 relevant as they influence normal (*Whittington et al., 2008*) and pathological (*Geertsen et al.,*
77 *2015*) gait mechanics.

78 Our understanding of how passive skeletal muscle force is affected in CHF is currently
79 unclear. Passive forces in cardiac muscle are altered in CHF (*Van der Velden, 2011*), as well as
80 in diaphragm skeletal muscle (*Van Hees et al., 2010*). Surprisingly, as far as we are aware, only
81 one study (*Van Hees et al., 2010*) has investigated passive forces in appendicular skeletal muscle
82 in CHF and it has been conducted in a mouse model. This study reported unaltered passive
83 forces in the soleus (SOL) muscle of CHF-affected mice, compared to a control group, when
84 taking into consideration muscle size.

85 The SOL has been identified as a primary muscle in which tissue loss occurs in CHF
86 (*Panizzolo et al., 2015; Green et al., 2016*) and its size is strongly correlated with the reduced
87 exercise capacity present in CHF (*Panizzolo et al., 2015*) (more so than the gastrocnemius
88 synergist). The SOL is also functionally relevant as it has been identified as the main source of
89 mechanical work during gait (*Mc Gowan et al., 2009*). Furthermore, the SOL permits an
90 estimation of passive force in a single muscle (*Rubenson et al., 2012; Tian et al., 2012*) and thus
91 is a muscle of choice for muscle-specific analysis.

92 Therefore, the aim of this study was to investigate the passive forces in the SOL muscle
93 of CHF patients and age- and physical activity-matched control participants, including their
94 relationship to muscle architecture [physiological cross sectional area (PCSA), muscle length,
95 pennation angle]. We hypothesized that there would be a reduction in passive force in CHF
96 patients, compared to a healthy population. We further hypothesized that passive force would be

97 similar after normalizing for the muscle PCSA, thus attributing alterations in passive force to
98 muscle size.

99

100 **MATERIALS AND METHODS**

101 **Participants**

102 Patients with CHF and age- and physical activity-matched control participants who were free
103 from other musculoskeletal disorders and lower limb musculoskeletal injuries were recruited for
104 this study. The CHF group included 12 participants (7 men, 5 women) in the class II-IV of the
105 New York Heart Association (NYHA) classification with an ejection fraction of $30.5 \pm 9.6\%$. (For
106 anthropometric characteristics and exclusion criteria see Table 1). The control group was
107 composed of 12 healthy participants recruited from the local community (8 men, 4 women). The
108 CHF group underwent regular exercise activity 2-3 times per week for ~ 1 hour per session
109 (treadmill walking and resistance weight training) as part of their standard patient care. The
110 control participants were selected from those reporting similar levels of weekly exercise,
111 assessed by means of a fitness questionnaire (*Godin & Shepard, 1985*). All participants read and
112 signed an informed consent prior to participating in the study and all of the procedures were
113 approved by the Human Research Ethics Committee at The University of Western Australia
114 (approval ID: RA/4/1/2533) and Royal Perth Hospital (approval ID: 2011/019).

115

116 **Passive force estimates**

117 The procedures used to estimate passive SOL forces were similar to those adopted previously
118 (*Rubenson et al., 2012*), with the exception that passive force was measured during continuous
119 joint rotation. Passive moments were recorded with the participants sitting upright with their

120 right foot and ankle positioned in a dynamometer (Biodex M3, Shirley, NY, USA) and with the
121 knee positioned at 120° of flexion (0° knee fully extended) to mitigate the force contribution of
122 the gastrocnemius muscles (*Maganaris, 2001*). The net passive ankle joint moment (M_p) was
123 computed by subtracting the moment generated by the Biodex rig and the weight of the foot
124 (*Rubenson et al., 2012*); the weight of the foot was expressed as a percentage of body mass. The
125 M_p over a joint's range of motion passes through zero at an angle that approximates where
126 passive muscle forces reach zero (*Silder et al., 2007*) (Figure 1). Moment data recorded by the
127 dynamometer were filtered using 4th-order zero-lag 2 Hz low-pass Butterworth filter (MATLAB,
128 The MathWorks Inc., USA). To detect the inflexion point in M_p where net dorsiflexion and
129 plantarflexion moment converge on zero we first fitted the joint angle vs. M_p data with a 5th-order
130 polynomial and subsequently computed the first order derivative of this function (MATLAB,
131 The MathWorks Inc., USA) (Figure 1).

132 Contribution from synergist muscles are minimal at the joint postures adopted
133 (*Maganaris, 2001; Silder et al. 2007; Rubenson et al., 2012*). This was confirmed from OpenSim
134 musculoskeletal models simulations (*Delp et al., 2007*) further indicating that passive force from
135 synergist muscles were minimal at the recorded knee and ankle postures. The method described
136 above does not account for passive moments arising from joint articulations and skin, but these
137 are minimal compared to the passive moments arising from passive force in the Achilles tendon
138 (*Costa et al., 2006*).

139 Electromyography (EMG) from the tibialis anterior (TA), the medial and lateral
140 gastrocnemius muscles (MG, LG, respectively) and the SOL were recorded during the trials
141 (Noraxon wireless system, Scottsdale, AZ, USA, 2000 Hz) to ensure the muscles crossing the
142 ankle remained inactive. For each trial, real-time root-mean-square (RMS) waves of the muscles'

143 activity were computed from the EMG signals (incorporating DC offset; Spike2 V7 software;
144 Cambridge Electronic Design, Cambridge, UK) (*Rubenson et al., 2012*). Soleus fascicle lengths
145 and pennation angle were recorded using dynamic B-mode ultrasound (Telemed, EchoBlaster
146 128, Lithuania; 25 Hz capture rate; 7.5 MHz 60 mm linear array probe) following the placement
147 and image analysis procedures outlined previously (*Rubenson et al., 2012; Panizzolo et al.,*
148 *2013*). Simultaneous measurements of ankle joint flexion/extension angles were made using a
149 portable 3D motion capture system (Optitrack, Corvallis, Oregon, US, 100 Hz). The net joint
150 moment, EMG, ultrasound images and joint angles were recorded synchronously (Micro1401-3;
151 Cambridge Electronic Design, Cambridge, UK; 2000 Hz) as the ankle was cycled through its full
152 range of motion (the most plantarflexed and most dorsiflexed position tolerated by the
153 participant) at a constant speed of 5°/s over three consecutive cycles.

154 Three initial warm-up cycles were performed prior the recording of any measurements.
155 The SOL passive force ($F_{p_{SOL}}$) was computed continuously throughout the joint range of motion
156 as the joint underwent dorsiflexion. Passive force was calculated as per (*Rubenson et al., 2012*)
157 using the following equation:

$$158 \quad F_{p_{SOL}} = \frac{M_p}{r * \cos \theta} \quad (1)$$

159 Where r represents the Achilles moment arm data and θ the SOL pennation angle, measured
160 according to (*Panizzolo et al., 2015*).

161 Participant-specific Achilles moment arm data were established experimentally on a
162 separate testing day, following the method described previously in (*Manal, Cowder &*
163 *Buchanan, 2010*). In this method B-mode ultrasound (Telemed, Echo Blaster 128, Lithuania)
164 was used to capture Achilles tendon images in the sagittal plane from the participants while their
165 foot was cycled passively at an angular velocity of 5°/s across its range of motion in a Biodex

166 dynamometer (M3, Biodex, Shirley, NY, USA). The ultrasound probe (7.5 MHz, 60 mm field of
167 view, linear array probe, 50 Hz capture rate) was placed longitudinally over the Achilles tendon,
168 so that the ankle joint was included in the field of view of the probe, using a stand-off gel pad
169 (Aquaflex, Parker, NJ, USA). Simultaneously, the trajectories of two retro-reflective markers
170 mounted on the ultrasound probe were recorded by means of a 3D motion capture system
171 (Optitrack, Corvallis, Oregon, US, 100 Hz). Additional anatomical landmarks (first metatarsal,
172 calcaneus, medial malleoli and knee medial condyle) were tracked to calculate the ankle
173 flexion/extension joint angle. A 2D customized graphical interface was developed in Matlab to
174 display both the ultrasound images and the ultrasound probe and the medial malleolus markers in
175 the same coordinate system. The line of action of the Achilles tendon was digitized in this
176 common coordinate system and the moment arm was computed as the perpendicular distance
177 between the midline of action of the tendon and the medial malleolus, which was used as an
178 estimate of the ankle joint center. This procedure was performed at 10 ankle joint angles that
179 spanned the joint's range of motion. A 10-point moment arm-joint angle curve was obtained for
180 each participant by using a polynomial fit of the moment arm-joint angle data.

181 We defined the fascicle slack length (L_{slack}) as the length where passive SOL forces are
182 first generated. L_{slack} was estimated as the point where the net passive dorsiflexion and
183 plantarflexion moments converge on zero (Figure 1). The fascicle length at the maximum
184 tolerated dorsiflexion angle was defined as the maximal fascicle length (L_{max}). Absolute and
185 normalized passive SOL force-length (F-L) curves were established for each participant.
186 Absolute passive F-L curves used the measured $F_{p_{SOL}}$ in Newtons and fascicle lengths (L) in mm.
187 Normalized passive F-L curves were created from absolute passive F-L curves by dividing each
188 participant $F_{p_{SOL}}$ by their SOL PCSA and by dividing L by L_{slack} (this normalized length is

189 referred as L_{norm} from hereinafter). The PCSA was determined from underwater 3D ultrasound
190 scans which allowed to obtain information relative to SOL muscle volume (Telemed,
191 EchoBlaster 128, Lithuania; Stradwin, Medical Imaging Research Group, Cambridge University
192 Engineering Department, UK) following (Panizzolo *et al.*, 2015). To enable the comparison of
193 absolute F_{pSOL} between groups, F_{pSOL} was determined at a percent fascicle stretch of 0%, 20%,
194 40%, 60%, 80% and 100% of the maximum fascicle stretch, where percent fascicle stretch was
195 defined as $((L - L_{slack}) \div (L_{max} - L_{slack})) * 100$. The same procedure was done to compare passive
196 moment data over both angle and muscle length ranges. Passive fascicle stiffness was computed
197 for each participant as the slope of the absolute F-L curves between L_{slack} and 40% stretch (k_1)
198 and between 60% - 100% stretch (k_2). In order to compare the normalized passive F-L curves we
199 evaluated the normalized F_{pSOL} at a set of L_{norm} between 1.0 and 1.4 (i.e. strain of 0 - 40%) using
200 intervals of 0.05. A peak L_{norm} was set to 1.4 as this represented the average maximum L_{norm} that
201 the participants achieved at their end range of ankle dorsiflexion. The normalized F_{pSOL} was
202 computed for each individual for the interval described above by fitting the normalized F_{pSOL} and
203 L_{norm} data using a 1st-order exponential equation (Gollapudi & Lin, 2009) with subject-specific
204 constants. In some circumstances where the set range exceeded the experimental L_{norm} the
205 normalized F_{pSOL} values were extrapolated from the exponential equation. Stiffness was
206 computed between L_{norm} of 1.0 and 1.2 (k_{1norm}) and 1.2 and 1.4 (k_{2norm}).

207

208 **Active forces estimates**

209 As an ancillary comparison of the muscle lengths, we also analyzed peak active muscle
210 forces at different ankle angles (and thus muscle lengths) to generate an active force-length

211 relationship. It has previously been shown experimentally, both in the human SOL muscle
212 (*Rubenson et al., 2012*) and in non-human muscle (*Azizi & Roberts, 2010*) that optimal muscle
213 lengths (L_0 ; lengths where peak active isometric forces are generated) correspond closely with
214 L_{slack} . Because of the importance of L_{slack} in our analyses of length-dependent passive muscle
215 force and muscle stiffness we chose to also assess L_0 as an additional test for differences in
216 fascicle lengths between groups. The main purpose of performing the active force-length curve
217 for the SOL muscle was thus to improve our assessment of length-dependent passive force and
218 muscle stiffness that relies on length normalization, rather than insights into active force
219 production *per se*.

220 The protocol used in this study to obtain predictions of moments and force generated by
221 the SOL (as well as the moments and force generated by synergist muscles and by the co-
222 contraction of dorsiflexor muscles) expands on the procedures established in (*Rubenson et al.,*
223 *2012*). It uses a combination of experimental net moment measurements from dynamometry,
224 ultrasound fascicle imaging, electromyography and a scaled participant-specific musculoskeletal
225 model in OpenSim 2.0.2 (*Delp et al., 2007*). Predictions were performed with the knee in a
226 flexed position ($>120^\circ$) and over a range of ankle angles from $\sim -20^\circ$ dorsiflexion to 30°
227 plantarflexion (the ankle range of motion varied between individuals ranging from individual
228 maximum dorsiflexion of -30° to individual maximal plantarflexion of nearly 50°). The muscle
229 length that corresponded with the maximal peak active force was designated as L_0 .

230 First, a generic OpenSim lower-limb model (*Arnold et al., 2010*) was scaled using each
231 participant's joint axes and centers determined via motion capture data (8-camera VICON MX
232 motion capture system, Oxford Metrics, UK; 100 Hz) from participants in a standing posture as
233 well as dynamic joint motions (*Besier et al., 2003*). From these trials, an inverse kinematics

234 algorithm was run on the position of 26 retroreflective spherical markers placed on anatomical
 235 landmarks and on functionally determined joint centers (*Besier et al., 2003*), that minimized the
 236 distance between the OpenSim model markers and the retroreflective and the functionally
 237 determined markers. These participants-specific models were positioned to match the
 238 participant's optically recorded ankle and knee joint posture and in turn used to predict M_{dorsi} and
 239 M_{Syn} (see below).

240 The moment generated by the plantarflexors (M_{plant}) during the maximal voluntary
 241 isometric plantarflexion contractions (MVC_{plant}) was calculated as:

$$242 \quad M_{plant} = M_{peak} - \Delta M_p + M_{dorsi} \quad (2)$$

243 where M_{peak} is the peak net ankle joint moment (calculated as the difference between the Biodex
 244 recorded moment during MVC_{plant} and the moment at rest), ΔM_p represents the difference in the
 245 estimated passive SOL moment during the MVC_{plant} and the passive SOL moment at rest prior to
 246 the contraction, and M_{dorsi} is the moment generated by the co-contraction of the dorsiflexors
 247 muscles.

248 ΔM_p was calculated as:

$$249 \quad \Delta M_p = \left(F_{pSOL}^{contr} * \cos \theta^{contr} * r^{contr} \right) - \left(F_{pSOL}^{rest} * \cos \theta^{rest} * r^{rest} \right) \quad (3)$$

250 where F_{pSOL} was obtained for both the fascicle length at the MVC_{plant} and the fascicle length
 251 during the rest period just prior to contraction using a linear interpolation of the passive F-L
 252 relationship (*rest* and *contr* superscripts designate rest or MVC_{plant} , respectively). r^{contr} was
 253 estimated by increasing the value predicted from the experimental Achilles moment arm- joint
 254 angle equation (described above) by 20% to take in account the increase in moment arm distance
 255 reported during MVC_{plant} with respect to length at rest (*Maganaris et al., 1998*).

256 The M_{dorsi} was predicted by the participant-specific OpenSim model. First, the OpenSim
257 maximal isometric forces of all the dorsiflexors (tibialis anterior, extensor digitorum longus,
258 extensor hallucis longus, peroneus tertius) were adjusted by the same percentage increase or
259 decrease so that the predicted model's peak isometric dorsiflexion moment at 100% activation (
260 MVC_{dorsi}) matched that of the participant's experimental maximum M_{dorsi} recorded in the Biodex
261 dynamometer at 10° plantarflexion, the angle that corresponds approximately to optimal
262 dorsiflexion moments (*Silder et al., 2007*). The MVC_{dorsi} were performed only at this joint angle
263 to reduce the total numbers of contractions performed and time spent in the experimental
264 protocol by each participant. This was an important consideration because of the general high
265 fatigability of CHF patients. In this procedure, the OpenSim model was positioned to match the
266 participant's optically recorded ankle and knee joint posture. In subsequent measurements of
267 MVC_{plant} the M_{dorsi} was predicted by the OpenSim model by prescribing an activation to all of the
268 dorsiflexors equal to the ratio of the TA's peak EMG (linear envelope) during the MVC_{plant} to its
269 peak EMG (linear envelope) from the MVC_{dorsi} trial; i.e. this assumed the same activation level
270 for all dorsiflexors.

271 To take into account the contribution of synergist muscles we predicted the relative
272 percentage contribution of each plantarflexors muscle to the total plantarflexor moment in
273 OpenSim (M_{syn}) by prescribing the recorded ankle and knee angles and 100% activation of all
274 plantarflexor muscles (peroneus longus, peroneus brevis, flexor hallucis, tibialis posterior, flexor
275 digitorum, MG, LG and SOL). The percent contribution of the OpenSim SOL to the total
276 predicted moment was applied to the experimental MVC_{plant} to define the moment generated by
277 the participant's SOL ($M_{a_{SOL}}$). Lastly, peak voluntary active SOL force production ($F_{a_{SOL}}$) was
278 calculated as:

279
$$F_{a_{SOL}} = \frac{M_{a_{SOL}}}{r^{contr} * \cos \theta^{contr}} \quad (4)$$

280 These active force trials were performed only by the participants that were able to tolerate
281 a prolonged protocol (n = 7 and n = 8, for control and CHF participants, respectively).

282

283 **Statistical analysis**

284 Differences in the absolute (non-normalized) passive moment-angle, moment-length and F-L
285 curves were assessed by testing if $F_{p_{SOL}}$ were different between groups (CHF and control), and if
286 joint angles at which the passive forces occurred and/or fascicle lengths were affected in the
287 CHF group, by using a two-way (CHF/control) repeated measures (0%, 20%, 40%, 60%, 80%
288 and 100% of angular excursion or muscle stretch, respectively) ANOVA, with Bonferroni *post*
289 *hoc* tests. Similar two-way repeated measures ANOVAs were also performed on the normalized
290 F-L curves using the L_{norm} set range (1.0 - 1.4). A two-tailed unpaired Student's t-test with
291 significance level of $p < 0.05$ was used to determine significant differences in the L_{slack} , L_{max} , the
292 maximal fascicle stretch, and L_0 , as well as in the passive fascicle stiffness (k_1 , k_2 , k_{1norm} and
293 k_{2norm}) and in the PCSA between the groups. Finally, we performed a linear regression analyses
294 between peak $F_{p_{SOL}}$ at L_{norm} of 1.4 and PCSA and between muscle volume across groups.
295 Statistical analysis was performed in SPSS (IBM, Statistics 21, USA).

296

297 **RESULTS**

298 No main effect of group was found in the joint angle between the CHF and control groups ($p =$
299 0.42) (Figure 2a). A main effect of group on net passive ankle joint moment was found ($p =$
300 0.01) with lower passive moment in the CHF group compared to the control group at relative

301 levels of angular excursion and fascicle stretch, although no statistically significant interaction
302 effect was found ($p = 0.40$) between group and joint angle (Figure 2a-b).

303 A main effect of group on absolute $F_{p_{SOL}}$ (N) was found ($p = 0.03$) with lower absolute
304 $F_{p_{SOL}}$ in the CHF group compared to the control group at relative levels of fascicle stretch,
305 although no statistically significant interaction effect was found ($p = 0.11$) between group and
306 level of stretch. No differences were found in k_1 and k_2 between the groups ($p = 0.32$; ES = 0.51
307 and $p = 0.85$; ES = 0.09) (Figure 3a), with stiffness exhibiting high variability. The L_{max} was
308 significantly shorter in the CHF group compared to the control group ($p = 0.046$; ES = 0.96),
309 although no statistically significant differences were found in L_{slack} ($p = 0.11$; ES = 0.76) and in
310 the maximal fascicle stretch ($L_{max} - L_{slack}$) ($p = 0.34$; ES = 0.44) (Table 2) or maximal fascicle
311 strain ($p = 0.70$; ES = 0.09).

312 A significantly smaller SOL PCSA was found in the CHF with respect to the control
313 group ($p = 0.02$; ES = 1.25) (Table 2). No main effect was found in the PCSA-normalized $F_{p_{SOL}}$
314 ($N\ cm^{-2}$) between the CHF and control groups when using the L_{norm} strain range of 1.0-1.4 ($p =$
315 0.46) (Figure 3b), nor was there an interaction effect between the PCSA-normalized $F_{p_{SOL}}$ and
316 normalized lengths ($p = 0.52$). Normalized passive fascicle stiffness (k_{1norm} and k_{2norm}) were
317 likewise variable and also not significantly different between the groups ($p = 0.42$; ES = 0.44 and
318 $p = 0.54$; ES = 0.33) (Figure 3b).

319 L_0 determined from the active force-length data was significantly shorter ($\sim 22\%$) in the
320 CHF group compared to the control group ($p = 0.04$; ES = 0.96) (Table 2). The maximal $F_{a_{SOL}}$
321 and corresponding L_0 occurred at approximately 10° dorsiflexion. The $F_{a_{SOL}}$ at both shorter and
322 longer fascicle lengths relative to L_0 decreased, characteristic of the muscle force-length

323 relationship (Figure 4). L_0 was not significantly different from L_{slack} in either the control or CHF
324 groups ($p = 0.33$ and $p = 0.39$, respectively; Table 2).

325 A significant correlation was found between peak $F_{p_{SOL}}$ at L_{norm} of 1.4 and muscle volume
326 ($p < 0.01$; $r = 0.76$) while no significant correlation was reported between peak $F_{p_{SOL}}$ at L_{norm} of
327 1.4 and PCSA ($p = 0.06$; $r = 0.46$).

328

329 **DISCUSSION**

330 The present study provides, to the best of our knowledge, the first estimate of *in vivo* passive
331 human skeletal muscle force-length properties in CHF. As predicted, higher absolute M_p and
332 $F_{p_{SOL}}$ were produced in the control group for a given amount of muscle stretch (Figure 2, 3).
333 However, and also in agreement with our hypothesis, passive force was not different after
334 normalizing by muscle PCSA, nor is passive muscle stiffness affected. These results indicate that
335 muscle size rather than intrinsic muscle properties is a major factor influencing passive forces in
336 CHF SOL muscle. This was further supported by the correlation between peak $F_{p_{SOL}}$ and muscle
337 size across both the CHF and control groups. This finding stands in contrast to previous work
338 reporting stiffer cardiac muscle due to alterations in the titin structure (*Wu, 2002*) or decreased
339 passive force of the diaphragm, due to titin loss (*Van Hees et al., 2010*) in CHF. On the other
340 hand, our results do corroborate data from passive skeletal muscle properties in the mouse SOL,
341 in which passive forces from CHF-affected animals were likewise not altered after normalizing
342 to muscle cross sectional area (*Van Hees et al., 2010*).

343 It was surprising, however, that for a given absolute muscle length, passive force was
344 significantly higher in CHF SOL compared to the control group. This unexpected finding stems
345 from the fact that over the same ankle range of motion the passive muscle lengths are shorter in

346 CHF patients, in particular at maximal stretch (Figure 2, 3). The result is that for the same
347 absolute muscle length (above L_{slack}) the CHF muscle has undergone greater strain, thus
348 generating greater force in titin and other passive load bearing muscle components. Previous
349 experimental studies (*Azizi & Roberts, 2010; Winters et al., 2011; Rubenson et al., 2012*) have
350 shown agreement between the onset of passive force generation (L_{slack}) and L_0 (optimal length for
351 active force production). The estimate of L_0 in the present study was similar to L_{slack} for both
352 groups but significantly ($p < 0.05$) shorter in the CHF group (Table 2). The shorter L_{slack} and L_0 in
353 CHF patients may indicate that the SOL has undergone a loss of in-series sarcomere numbers, a
354 contributing factor to the reduced muscle size (*Panizzolo et al., 2015*). It was also surprising that,
355 despite their shorter muscle fascicles, CHF patients underwent the same ankle range of motion
356 and a similar SOL muscle strain across this range of motion (Figure 2, Table 2). Therefore, the
357 ‘effective’ stiffness of the muscle, the amount of force resulting at the maximal stretch of the
358 muscle (as indicated by k_1 and k_2), are similar between groups despite the passive force at the
359 same absolute muscle length being substantially greater in CHF patients. The passive moments at
360 equivalent ankle angle excursions (indicative of the ankle’s effective angular stiffness) are
361 likewise similar between CHF and control groups (Figure 2). This is true except for a moderately
362 higher moment, and absolute force, in the control group at the participant’s peak dorsiflexion
363 angle (Figure 2, 3) although these angles are rarely achieved during normal movement tasks. The
364 Achilles moment arms were similar between the control and CHF group suggesting that greater
365 Achilles strain might explain the similarity in joint and muscle excursions. This is partially
366 supported by the smaller tendon cross sectional area reported in CHF (*Panizzolo et al., 2015*).

367

368 **Functional implications**

369 Our results are consistent with the observation that muscle size dictates functional deficits in
370 CHF (*Magnusson et al., 1994*). Exercise that promotes hypertrophy should therefore be a focus
371 for restoring functional capacity in leg muscles. Exercise prescription for CHF is becoming
372 commonplace, but programs that include specifically designed lower limb resistance training
373 might be especially promising (*Maiorana et al., 2000*).

374 Our results also offer insight into the gait mechanics of CHF patients (*Panizzolo et al.,*
375 *2014*). The combination of the shorter SOL muscle fascicles in CHF patients and their greater
376 dorsiflexion during mid-stance of gait (*Panizzolo et al., 2014*) may cause significantly greater
377 SOL strain. This might lead to the muscle operating on to the descending limb of the F-L curve
378 where large passive forces develop (*Rassier, MacIntosh & Herzog., 1999; Rubenson et al.,*
379 *2012*). In this scenario CHF patients would rely more on their passive forces to support the
380 plantarflexion moment during walking, which has the benefit of reducing metabolically
381 expensive active force development. This may help explain why CHF patients rely
382 proportionately more on their ankle for powering walking as speed and metabolic demand
383 increases (*Panizzolo et al., 2014*). However, whilst metabolically advantageous, this mechanism
384 might lead to greater lengthening-induced muscle damage. Alternatively, a larger dorsiflexion
385 during the stance phase could be explained by a higher tendon strain, without affecting the SOL
386 strain itself. The muscle's F-L operating range and its interplay with the Achilles tendon function
387 depend on multiple factors, including tendon stiffness and a detailed understanding will require
388 further *in vivo* analyses to clarify the underlying mechanism.

389

390 **Limitations**

391 Some limitations of the present study need to be acknowledged. First, in the measurement of M_p
392 used to calculate passive forces estimates, some participants displayed an inflection point (where
393 net dorsiflexion and plantarflexion moment converge on zero, Figure 1) slightly above or below
394 zero moment (<1.5 Nm or ~7% of the peak passive moment). This can occur if the weight of the
395 leg transmits a small moment about the Biodex axis (i.e. small misalignment of ankle center of
396 rotation) or if the moment predicted from the weight of the foot has small errors. In these cases
397 the passive moment data was corrected for the offset. Second, the method used to calculate the
398 Achilles moment arm data (*Manal et al., 2010*), assumed the position of the ankle joint center
399 coincides with the marker placed on the medial malleolus. This could have resulted in a potential
400 misalignment of the ankle joint center, which might have affected the estimation of the moment
401 arm measurements. Investigations have also shown that muscle fascia structure can act as a
402 pathway for myofascial force transmission (*Purslow et al. 2010*), thus making more difficult to
403 completely isolate fascicle force production at single muscle level. Nevertheless, this factor has
404 been reported to be relatively small in intact muscles (*Maas & Sundercock, 2010*) and most
405 likely did not significantly impacted our findings. Lastly, the heterogeneity of the CHF group
406 needs to be acknowledged as it might have influenced some of the findings. The difficulty
407 associated with enrolling large numbers of CHF participants to undertake prolonged
408 biomechanical tests prevented us from controlling for variables such as body mass, composition,
409 stature, or sex. Nevertheless, we tried to mitigate this problem by recruiting closely matched age
410 and physical activity-level control participants.

411

412 CONCLUSION

413 This work suggests that a primary factor leading to lower passive forces in the SOL is likely a
414 reduction in muscle size. However, shorter muscle fascicles in CHF results in greater passive
415 forces for a given absolute muscle length, and might be linked to changes in CHF gait (*Panizzolo*
416 *et al.*, 2014). Exercise that promotes calf muscle hypertrophy and serial sarcomerogenesis may
417 prove particularly beneficial in CHF patients.

418

419 ACKNOWLEDGEMENTS

420 The authors would like to acknowledge Ms. Kirsty McDonald and Ms. Maddison Jones for their
421 help during data collection, and all of the participants who volunteered for this study.

422

423

424 REFERENCES

425 Anker SD, Ponikowski PP, Clark AL, Leyva F, Rauchhaus M, Kemp M, Teixeira MM,
426 Hellewell PG, Hooper J, Poole-Wilson PA, Coats AJ. Cytokines and neurohormones relating
427 to body composition alterations in the wasting syndrome of chronic heart failure. *Eur Heart*
428 *J.* 1999; 20: 683–693.

429

430 Arnold EM, Ward SR, Lieber RL, Delp SL. A model of the lower limb for analysis of human
431 movement. *Ann Biomed Eng.* 2010; 38: 269-279.

432

433 Azizi E, Roberts TJ. Muscle performance during frog jumping: influence of elasticity on
434 muscle operating lengths. *Proc Biol Sci.* 2010; 277: 1523–1530.

435

436 Besier TF, Sturnieks DL, Alderson JA, Lloyd DG. Repeatability of gait data using a
437 functional hip joint centre and a mean helical knee axis. *J Biomech.* 2003; 36: 1159-1168.

438

439 Chua TP, Anker SD, Harrington D, Coats AJ. Inspiratory muscle strength is a determinant of
440 maximum oxygen consumption in chronic heart failure. *Br Heart J.* 1995; 74: 381–385.

441

442 Costa ML, Logan K, Heylings D, Donell ST, Tucker K. The effect of Achilles tendon
443 lengthening on ankle dorsiflexion: a cadaver study. *Foot Ankle Int.* 2006; 27: 414-417.

444

445 Delp SL, Anderson FC, Arnold AS, Loan P, Habib A, John CT, Guendelman E, Thelen DG.
446 OpenSim: open-source software to create and analyze dynamic simulations of movement.
447 *IEEE Trans Biomed Eng.* 2007; 54: 1940–1950.

448

449 Fülster S, Tacke M, Sandek A, Ebner N, Tschöpe C, Doehner W, Anker SD, von Haehling S.
450 Muscle wasting in patients with chronic heart failure: results from the studies investigating
451 co-morbidities aggravating heart failure (SICA-HF). *Eur Heart J.* 2013; 34: 512–519.

452

453 Geertsen SS, Kirk H, Lorentzen J, Jorsal M, Johansson CB, Nielsen JB. Impaired gait
454 function in adults with cerebral palsy is associated with reduced rapid force generation and
455 increased passive stiffness. *Clin Neurophysiol.* 2015; 126: 2320-2329.

456

457 Gollapudi SK, Lin DC. Experimental determination of sarcomere force-length relationship in
458 type-I human skeletal muscle fibers. *J Biomech.* 2009; 42: 2011-2016.

459

460 Godin G, Shepard RJ. A simple method to assess exercise behavior in the community. *Can J*
461 *Appl Sport Sci.* 1985; 10:141-146.

462

463 Green DJ, Panizzolo FA, Lloyd DG, Rubenson J, Maiorana AJ. Soleus muscle as a surrogate
464 for health status in human heart failure. *Exerc Sport Sci Rev.* 2016; 44:45-50.

465

466 Harrington D, Anker SD, Chua TP, Webb-Peploe KM, Ponikowski PP, Poole-Wilson PA,
467 Coats AJ. Skeletal muscle function and its relation to exercise tolerance in chronic heart
468 failure. *J Am Coll Cardiol.* 1997; 30: 1758–1764.

469

470 Maas H, Sandercock TG. Force transmission between synergistic skeletal muscles through
471 connective tissue linkages. *J Biomed Biotechnol.* 2010; Article ID 575672.

472

473 Maganaris CN, Baltzopoulos V, Sargeant AJ. Changes in Achilles tendon moment arm from
474 rest to maximum isometric plantarflexion: in vivo observations in man. *J Physiol.* 1998; 510:
475 977–985.

476

477 Maganaris CN. Force-length characteristics of in vivo human skeletal muscle. *Acta Physiol*
478 *Scand.* 2001; 172: 279–285.

479

480 Magnusson G, Isberg B, Karlberg KE, Sylvén C. Skeletal muscle strength and endurance in
481 chronic congestive heart failure secondary to idiopathic dilated cardiomyopathy. *Am J*
482 *Cardiol.* 1994; 73: 307–309.

483

484 Maiorana A, O’Driscoll G, Cheetham C, Collis J, Goodman C, Rankin S, Taylor R, Green D.
485 Combined aerobic and resistance exercise training improves functional capacity and strength
486 in CHF. *J Appl Physiol.* 2000; 88: 1565–1570.

487

488 Manal K, Cowder JD, Buchanan TS. A hybrid method for computing achilles tendon
489 moment arm using ultrasound and motion analysis. *J Appl Biomech.* 2010; 26: 224–228.

490

491 Mancini DM, Walter G, Reichek N, Lenkinski R, McCully KK, Mullen JL, Wilson JR.
492 Contribution of skeletal muscle atrophy to exercise intolerance and altered muscle
493 metabolism in heart failure. *Circulation.* 1992; 85: 1364–1373.

494

495 McGowan CP, Kram R, Neptune RR. Modulation of leg muscle function in response to
496 altered demand for body support and forward propulsion during walking. *J Biomech.* 2009;
497 42: 850–856.

498

499 Minotti JR, Pillay P, Oka R, Wells L, Christoph I, Massie BM. Skeletal muscle size:
500 relationship to muscle function in heart failure. *J Appl Physiol.* 1993; 75: 373–381.

501

502 Oskouei MA, Van Mazijk BC, Schuiling MH, Herzog W. Variability in the interpolated
503 twitch torque for maximal and submaximal voluntary contractions. *J Appl Physiol.* 2003; 95:
504 1648-1655.

505
506 Panizzolo FA, Green DJ, Lloyd DG, Maiorana AJ, Rubenson J. Soleus fascicle length
507 changes are conserved between young and old adults at their preferred walking speed. *Gait*
508 *Posture.* 2013; 38: 764–769.

509
510 Panizzolo FA, Maiorana AJ, Naylor LH, Dembo L, Lloyd DG, Green DJ, Rubenson J. Gait
511 analysis in chronic heart failure: the calf as a locus of impaired walking capacity. *J Biomech.*
512 2014; 47: 3719-3725.

513
514 Panizzolo FA, Maiorana AJ, Naylor LH, Lichtwark GA, Dembo L, Lloyd DG, Green DJ,
515 Rubenson J. Is the soleus a sentinel muscle for impaired exercise capacity in heart failure ?
516 *Med Sci Sport Exerc.* 2015; 47: 498-508.

517
518 Pincivero DM, Green RC, Mark JD, Campy RM. Gender and muscle differences in EMG
519 amplitude and median frequency, and variability during maximal voluntary contractions of
520 the quadriceps femoris. *J Electromyography Kines.* 2000; 10: 189-196.

521
522 Rassier DE, MacIntosh BR, Herzog W. Length dependence of active force production in
523 skeletal muscle. *J Appl Physiol.* 1999; 86: 1445-1457.

524

525 Purslow PP. Muscle fascia and force transmission. *J Bodyw Mov Ther.* 2010; 14:411-417.

526

527 Rubenson J, Pires NJ, Loi HO, Pinniger GJ, Shannon DG. On the ascent: the soleus operating
528 length is conserved to the ascending limb of the force-length curve across gait mechanics in
529 humans. *J Exp Biol.* 2012; 215: 3539–3551.

530

531 Silder A, Whittington B, Heiderscheit B, Thelen DG. Identification of passive elastic joint
532 moment-angle relationships in the lower extremity. *J Biomech.* 2007; 40: 2628–2635.

533

534 Sunnerhagen KS, Cider Å, Schaufelberger M, Hedberg M, Grimby G. 1998. Muscular
535 performance in heart failure. *J Card Fail.* 1998; 4: 97–104.

536

537 Tian M, Herbert RD, Hoang P, Gandevia SC, Bilston LE. Myofascial force transmission
538 between the human soleus and gastrocnemius muscles during passive knee motion. *J Appl*
539 *Physiol.* 2012; 113: 517-523.

540

541 Toth MJ, Ades PA, Tischler MD, Tracy RP, LeWinter MM. Immune activation is associated
542 with reduced skeletal muscle mass and physical function in chronic heart failure. *Int J*
543 *Cardiol.* 2006; 109: 179–187.

544

545 Toth MJ, Shaw AO, Miller MS, VanBuren P, LeWinter MM, Maughan DW, Ades PA.
546 Reduced knee extensor function in heart failure is not explained by inactivity. *Int J Cardiol.*
547 2010; 143: 276–282.

548

549 Van der Velden J. Diastolic myofilament dysfunction in the failing human heart. *Pflugers*
550 *Arch.* 2011; 462: 155–163.

551

552 Van Hees HW, Ottenheijm CA, Granzier HL, Dekhuijzen PN, Heunks LM. Heart failure
553 decreases passive tension generation of rat diaphragm fibers. *Int J Cardiol.* 2010; 141: 275–
554 283.

555

556 Volterrani M, Clark AL, Ludman PF, Swan JW, Adamopoulos S, Piepoli M, Coats AJ.
557 Predictors of exercise capacity in chronic heart failure. *Eur Heart J.* 1994; 15, 801–809.

558

559 Whittington B, Silder A, Heiderscheit B, Thelen DG. The contribution of passive-elastic
560 mechanisms to lower extremity joint kinetics during human walking. *Gait Posture.* 2008; 27,
561 628–634.

562

563 Winters TM, Takahashi M, Lieber RL, Ward, S.R. Whole muscle length-tension
564 relationships are accurately modeled as scaled sarcomeres in rabbit hindlimb muscles. *J*
565 *Biomech.* 2011; 44: 109–115.

566

567 Wu Y. Changes in titin isoform expression in pacing-induced cardiac failure give rise to
568 increased passive muscle stiffness. *Circulation.* 2002; 106: 1384–1389.

Figure 1

Net passive ankle joint moment-angle relationship for one representative participant.

The measured moment is displayed with solid black line, the 5th-order polynomial fit with dashed black line, the inflexion point where net dorsiflexion and plantarflexion moment converge on zero is displayed with a black circle (○)

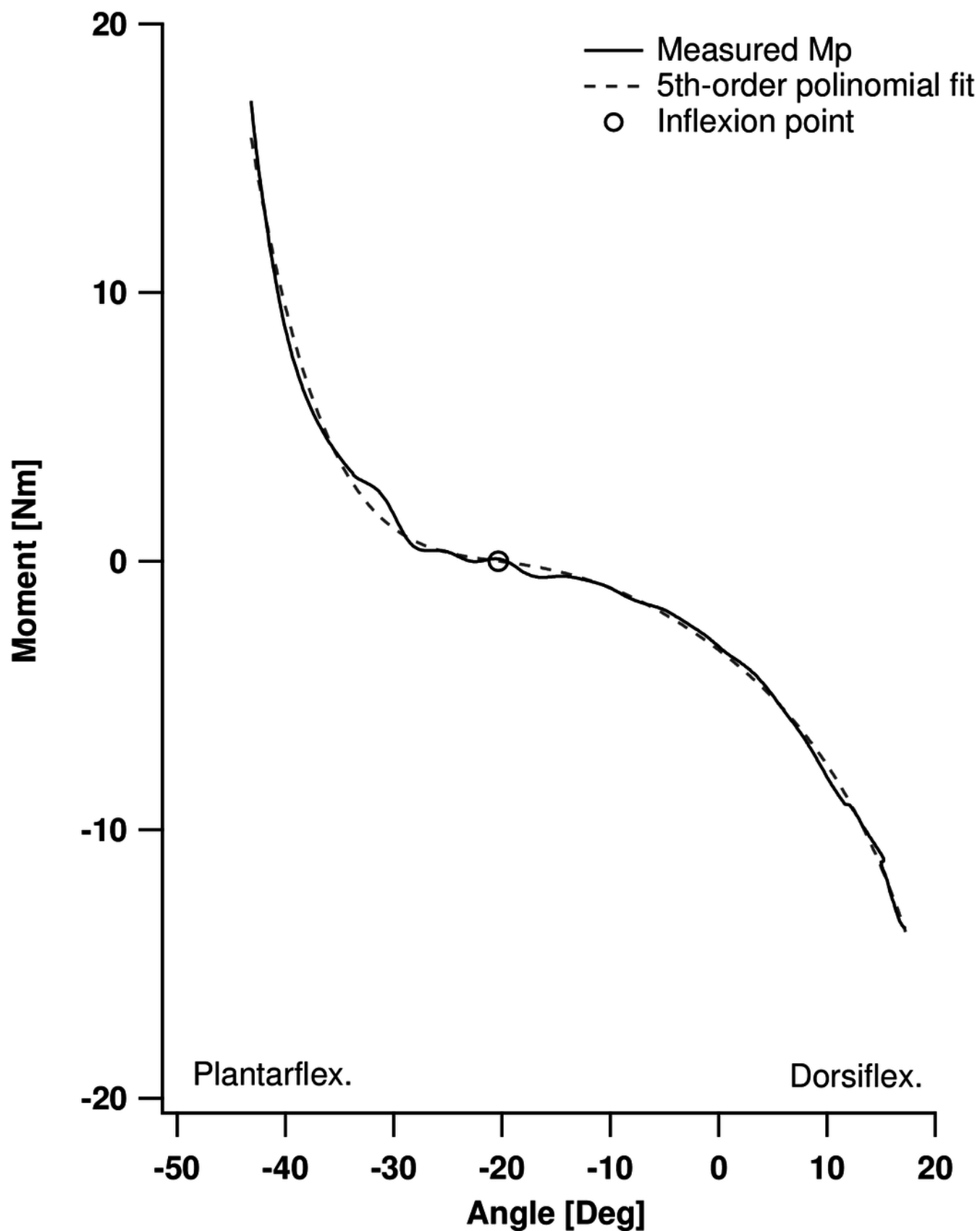


Figure 2

Soleus passive moment-angle relationship (evaluated at 0%, 20%, 40%, 60% and 100% of the angle's maximal dorsiflexion) (a) and passive moment-length relationship (b).

The chronic heart failure (CHF) group is displayed in grey triangles (\blacktriangle), and control group in black circles (\bullet). Average curves are displayed \pm S.D. * designates a statistical difference in passive moment between groups (ANOVA main effect; $p < 0.05$; CHF vs. control)

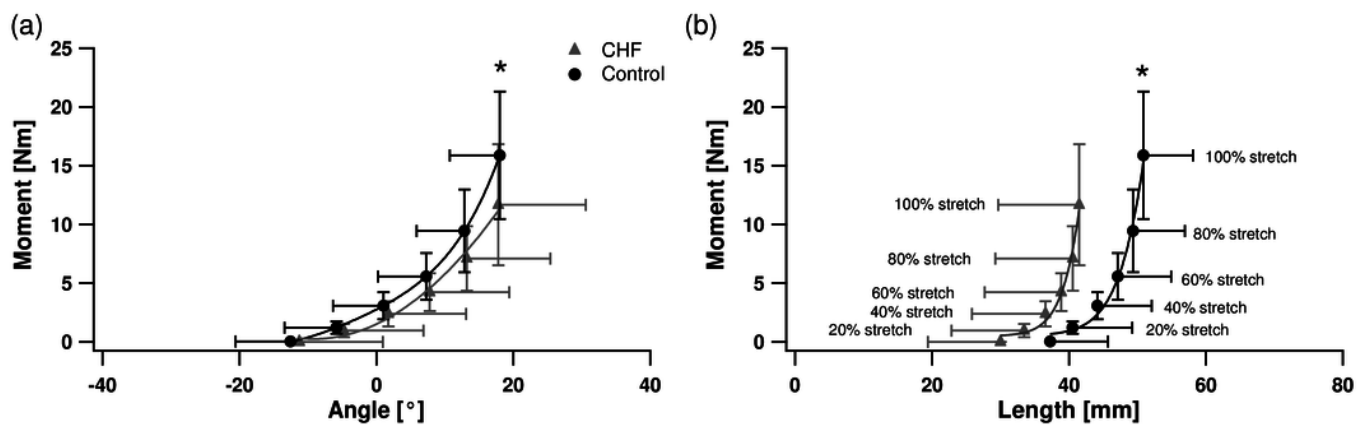


Figure 3

Soleus Passive force-length (F-L) relationship (a) and passive F-L relationship normalized by individual PCSA and L_{slack} (b).

Passive F-L is evaluated at 0%, 20%, 40%, 60% and 100% of the muscle's maximal stretch (a), passive F-L is evaluated at L_{norm} between 1.0 - 1.4 (b). The chronic heart failure (CHF) group is displayed in grey triangles (\blacktriangle), and control group in black circles (\bullet). Average curves are displayed \pm S.D. * designates a statistical difference in passive force between groups (ANOVA main effect; $p < 0.05$; CHF vs. control). # designates a significant difference in maximal passive fascicle length (L_{max}) between groups ($p < 0.05$; CHF vs. control)

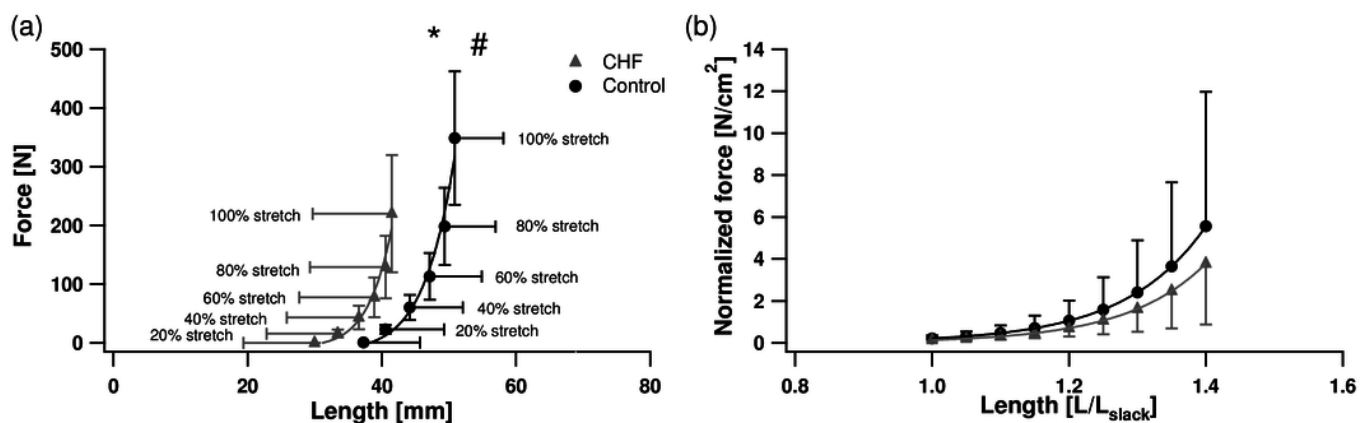


Figure 4

Normalized soleus peak voluntary force production and fascicle length.

Peak voluntary force production is normalized by the individual's maximal peak voluntary force production ($F_{a_{SOL}}$) while fascicle length is expressed in mm. Data points (mean \pm S.D.) include measurements taken at joint angles greater and less than 10° dorsiflexion. Muscle lengths were grouped in four clusters equally spaced along the fascicle length range. A data point at ($L_0, 1$) is included for reference purposes only. The chronic heart failure (CHF) group is displayed by grey triangles (\blacktriangle), and control group by black circles (\bullet)

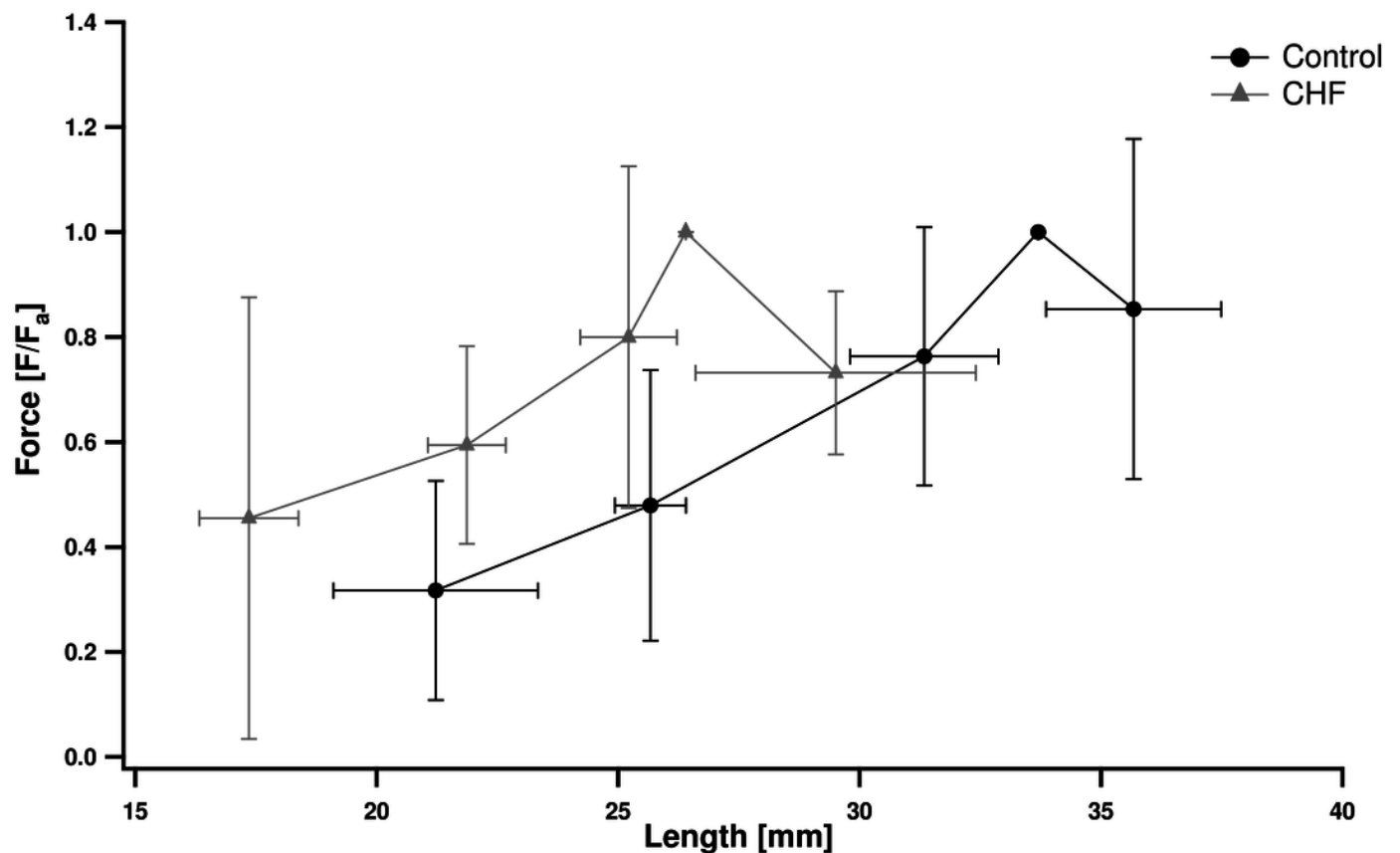


Table 1 (on next page)

Anthropometric characteristics of the participants involved in the study. Data are means \pm SD

Criteria for exclusion for the CHF group included severe renal (creatinine >250 mmol/l or eGFR <30 ml/min/1.73 m²) or hepatic (bilirubin >50 mmol/l) dysfunction or unexplained anemia (hemoglobin <100 g/l) or thrombocytopenia (platelets $<100 \times 10^9$ /l). Participants with the following contra-indications to exercise were excluded: unstable angina or exercise-induced ischemia at low exercise levels (less than three metabolic equivalent units), severe aortic stenosis, severe mitral or aortic regurgitation, or hypertrophic cardiomyopathy

1 **Table 1**

Group	Age [yr]	Height [cm]	Weight [kg]
Control	62.7±5.6	173.3±6.1	69.7±8.5
CHF	63.5±10.9	168.2±9.6	67.9±14.8

2

3

4

5

6

Table 2 (on next page)

Muscle parameters. Data are means \pm SD

*indicates a significant difference ($p < 0.05$)

1 **Table 2**

SOL muscle parameter	CHF	Control
L_{slack} [mm]	30.0±10.6	37.3±8.4
L_{max} [mm]	41.5±11.8*	50.9±7.3
$L_{max} - L_{slack}$ [mm]	11.5±5.2	13.6±4.2
L_0 [mm]	26.4±6.4*	33.7±8.4
Max strain (L_{norm})	1.4±0.2	1.4±0.2
PCSA [cm ²]	65.0±13.0*	91.0±20.5
Max $F_{p_{SOL}}$ [N]	220.0±99.6*	348.6±113.4
k_1 [N/mm]	6.9±2.9	12.0±13.8
k_2 [N/mm]	75.1±78.9	82.6±85.7
k_{1norm}	2.8±1.7	4.1±4.1
k_{2norm}	18.0±14.8	26.3±32.2

2